

Tunneling from a correlated 2D electron system transverse to a magnetic field

T. Sharpee^(a), M.I. Dykman^(a), and P.M. Platzman^(b)

^(a)*Department of Physics and Astronomy, Michigan State University, East Lansing, Michigan 48824*

^(b)*Bell Laboratories, Lucent Technologies, Murray Hill, New Jersey 07974*

(November 1, 2018)

We show that, in a magnetic field parallel to the 2D electron layer, strong electron correlations change the rate of tunneling from the layer exponentially. It results in a specific density dependence of the escape rate. The mechanism is a dynamical Mössbauer-type recoil, in which the Hall momentum of the tunneling electron is partly transferred to the whole electron system, depending on the interrelation between the rate of interelectron momentum exchange and the tunneling duration. We also show that, in a certain temperature range, magnetic field can *enhance* rather than suppress the tunneling rate. The effect is due to the magnetic field induced energy exchange between the in-plane and out-of-plane motion. Magnetic field can also induce switching between intra-well states from which the system tunnels, and a transition from tunneling to thermal activation. Explicit results are obtained for a Wigner crystal. They are in qualitative and quantitative agreement with the relevant experimental data, with no adjustable parameters.

PACS numbers: 73.40.Gk, 73.50.-h, 73.20.Dx, 73.50.Jt

I. INTRODUCTION

Many properties of low density two-dimensional electron systems (2DES) are strongly influenced by electron correlations [1]- [3]. Tunneling is one of the most direct tools for revealing these correlations, as has been demonstrated for systems which display the quantum Hall effect [4]. In this paper we show that tunneling can directly reveal correlations in a totally different class of systems, the low-density 2DES which are far away from the quantum Hall regime. This happens for tunneling not *into* the 2DES, but *from* the 2DES into the volume, and for a magnetic field \mathbf{B} applied *parallel* rather than perpendicular to the electron layer. The effect may not be described in terms of a phenomenological tunneling Hamiltonian: it is the tunneling matrix element itself that is sensitive to the electron correlations. As we show, it depends strongly, and very specifically, on electron density, and also on temperature and the magnetic field. An exponentially strong deviation of the tunneling exponent in a magnetic field from the predictions of the single-electron theory have been observed for a 2DES on helium [5]. However, these observations remained unexplained.

The field \mathbf{B} parallel to a 2DES couples the out-of-plane tunneling motion of an electron to the in-plane motion. For an isolated electron, which is separated from the continuum by a 1D potential barrier $U(z)$, see Fig. 1, and is free to move in the plane (x, y) , this results in an exponential suppression of the rate of tunneling decay. Indeed, when the electron moves by a distance z away from the layer, it acquires the in-plane Hall velocity $\mathbf{v}_H = (e/c)\mathbf{B} \times \mathbf{z}$. The corresponding kinetic energy $m\mathbf{v}_H^2/2 \equiv m\omega_c^2 z^2/2$ is subtracted from the energy of the out-of-plane tunneling motion ($\omega_c = |eB|/mc$ is the cyclotron frequency), or equivalently, there emerges

a “magnetic barrier” $m\omega_c^2 z^2/2$. This leads to a sharp decrease of the decay rate.

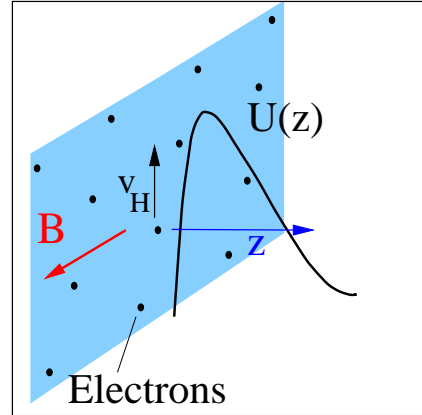


FIG. 1. The geometry of tunneling from a correlated 2DES transverse to a magnetic field; ω_p is the characteristic in-plane vibration frequency.

The electron-electron interaction can totally change the above picture. If the electron system is spatially correlated, forming a Wigner crystal (WC) or a correlated electron liquid, see Fig. 1, the tunneling electron transfers a part of its in-plane Hall momentum to other electrons. This decreases the loss of the energy for out-of-plane tunneling motion [6]. The mechanism is similar to that of the Mössbauer effect where the momentum of a gamma quantum is given to the crystal as a whole. However, in the present case the *dynamics* of the interelectron momentum exchange is very substantial. The characteristic momentum exchange rate is given by the zone-boundary plasma frequency ω_p , which is related to the electron density n by $\omega_p = (2\pi e^2 n^{3/2}/m)^{1/2}$. If ω_p exceeds the recip-

rocal duration of underbarrier motion in imaginary time τ_f^{-1} , the WC momentum adiabatically follows that of the tunneling electron. As a result, the Hall velocity is the same for all electrons, and $v_H \propto 1/N \rightarrow 0$ (N is the number of electrons). The effect of the magnetic field on tunneling is then fully compensated. For $\omega_p \tau_f \sim 1$ the compensation is only partial. One can say that tunneling is accompanied by creation of phonons of the WC, and the associated energy goes towards the magnetic barrier. However, the barrier turns out to be smaller than for a free electron, and the tunneling rate is then exponentially larger. Still, for $T = 0$ it is much smaller than for $B = 0$.

We show in this paper, that unexpectedly, in a certain temperature range the B -induced suppression of the rate of tunneling from a 2DES may be reversed, and then the decay rate exponentially increases with B . This happens because thermal energy of the in-plane electron motion is transferred by the magnetic field into the energy of tunneling motion. Although the effect is generic, as we show below, it does not arise in systems where the tunneling rate can be found using the instanton (bounce) technique [7], which is traditionally applied to describe tunneling for $B = 0$ [8]. There are two reasons which require to modify this technique. First, the magnetic field breaks time-reversal symmetry, and therefore, except for the case where the Hamiltonian of the system has a special form [9], there are no escape trajectories in real space and imaginary time, and the system comes out from the barrier with a finite velocity [10]. Second, for 2D systems the confining potential $U(z)$ is usually nonparabolic near the minimum, and even nonanalytic, with a step in the case of heterostructures and, in the case of electrons on helium, the singularity of the image potential. Therefore such systems are good candidates for observing magnetic field enhancement of the tunneling rate.

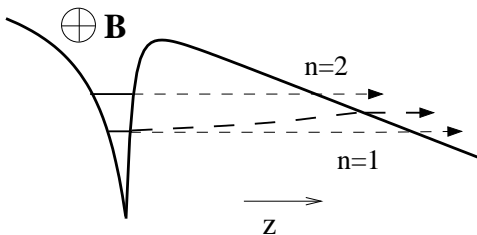


FIG. 2. Energy transfer from thermal in-plane motion into out-of-plane tunneling motion induced by the magnetic field (schematically).

The crossover from suppression to enhancement of tunneling by the field occurs for a temperature T_c which is of the order of the reciprocal imaginary duration of underbarrier motion τ_0^{-1} for $B = 0$ in the ground electron state [in what follows we use units where $\hbar = k_B = 1$]. If the tunneling rate for $B = 0$ is written as $W_0 \propto \exp[-2S_0]$, then $\tau_0 = \partial S_0 / \partial E_g$, where E_g is the ground-state energy of out-of-plane motion in the potential well of $U(z)$.

The tunneling probability increases if the in plane energy E_{plane} is transferred by the magnetic field into the tunneling energy E_g , at least in part, as illustrated in Fig. 2. The probability to have an energy E_{plane} is $\propto \exp(-E_{\text{plane}}/T)$. Therefore the overall probability, which is determined by the product of the two probabilities, depends on the interrelation between T and τ_0 .

The time τ_0 also often determines the temperature T_a for which there occurs a crossover from tunneling decay to decay via activated overbarrier transitions for $B = 0$ [11,12]. Therefore T_a and T_c are of the same order of magnitude. The interrelation between these temperatures is determined by the parameters of the system, and various interesting situations may occur depending on these parameters, as we discuss below. For example, the logarithm of the escape rate may increase with B even for $T > T_a$, because in a certain B -range, the rate of tunneling from the ground state exceeds the activation rate, even though it is smaller than the activation rate for $B = 0$. Similarly, with increasing B there may occur switching from tunneling from the excited intrawell states (see Fig. 2) to tunneling from the ground state.

For $T < T_c$, on the other hand, the tunneling rate decreases with the increasing B . However, for large enough B this increase stops, and escape occurs via thermal activation.

Explicit results on the effect of electron correlations on tunneling will be obtained assuming that electrons form a Wigner crystal. Because of strong correlations, overlapping of the wave functions of individual electrons is small, and electrons can be “identified”. The problem is then reduced to the tunneling of an electron coupled to in-plane vibrations of the Wigner crystal. As we will see, the results provide a good approximation also for a correlated electron liquid.

In Sec. II we formulate the model. In Sec. III we obtain the general expression for the tunneling rate in the WKB approximation, with account taken of the discreteness of the energy spectrum of electron motion transverse to the layer. The result can be understood in terms of the tunneling trajectory where the duration of motion transverse to the layer (in imaginary time) is not fixed, it has to be found and depends on temperature and the magnetic field. In Sec. IV we analyze the tunneling exponent, including the case of $T = 0$. In Sec. V we discuss temperature effects and show the possibility of B -induced enhancement of tunneling and of switching between different regimes of escape from the potential well. In Sec. VI explicit results are obtained using the Einstein model of the Wigner crystal in which all phonons are assumed to have the same frequency. Explicit expressions are obtained for a triangular and square tunneling barriers. In Sec. VII we apply the results to electron tunneling from helium surface and provide a detailed comparison with the experimental data [5]. Sec. VIII contains concluding remarks.

II. THE MODEL

A 2D electron system displays strong correlations if the ratio Γ of characteristic Coulomb energy of the electron-electron interaction $e^2(\pi n)^{1/2}$ to the characteristic kinetic energy is large (here, n is the electron density). In degenerate systems the kinetic energy is the Fermi energy $\pi n/m$, whereas in nondegenerate systems it is the thermal energy T . An example of a strongly correlated nondegenerate 2DES is electrons on helium. The experimental data for this system refer to the range $\Gamma > 20$ [2]. A classical transition to a Wigner crystal (WC) was observed for $\Gamma \approx 130$ [13,14]. Recently much attention have attracted also strongly correlated low-density electron and hole systems in semiconductors, where there have been reached the values of $\Gamma \sim 40$ which are expected to be sufficient for Wigner crystallization in a degenerate system [1].

The effect on tunneling of the magnetic field \mathbf{B} parallel to the electron layer is most pronounced if the tunneling length L is long, because the in-plane Hall momentum due to tunneling $m\omega_c L$ is simply proportional to L . Respectively, of utmost interest to us are systems with broad and comparatively low barriers. Yet in experimental systems the barrier widths are most likely to be less than 10^3 \AA . Therefore, in order to somewhat simplify the analysis we will assume (although this is not substantial) that L is less than the average inter-electron distance $\sim n^{-1/2}$. In this case, since electrons in a strongly correlated system stay away from each other, the in-plane electron dynamics only weakly affects the tunneling potential [15]. We will neglect the corresponding coupling for $B = 0$. The major effect on tunneling comes from a few nearest neighbors, and the presence or absence of long-range order in the 2DES does not affect the tunneling rate. Therefore we will analyze tunneling assuming that the electron system is a Wigner crystal. As we will see, the results will indeed depend on the short-wavelength modes of the WC, as expected from the above arguments, and therefore we believe that the model provides a good approximation even where electrons form a correlated fluid.

In a strongly correlated system, exchange effects are not significant, and one can identify the tunneling electron. Its out-of-plane motion for $B = 0$ is described by the Hamiltonian

$$H_0 = \frac{p_z^2}{2m} + U(z). \quad (1)$$

The potential $U(z)$ has a well which is separated by a tunneling barrier from the extended states with a quasi-continuous spectrum, cf. Fig. 1. The well is nonparabolic near the minimum, in the general case. The metastable intrawell states are quantized. We will consider temperatures for which nearly all electrons are in the lowest level, with energy E_g .

The magnetic field \mathbf{B} parallel to the layer mixes the out-of-plane motion of the tunneling electron with the in-plane vibrations of the Wigner crystal. The full Hamiltonian is of the form

$$H = H_0 + H_B + H_v, \quad (2)$$

with

$$H_v = \frac{1}{2} \sum_{\mathbf{k}, j} [m^{-1} \mathbf{p}_{\mathbf{k}j} \mathbf{p}_{-\mathbf{k}j} + m\omega_{\mathbf{k}j}^2 \mathbf{u}_{\mathbf{k}j} \mathbf{u}_{-\mathbf{k}j}] \quad (3)$$

and

$$H_B = \frac{1}{2} m\omega_c^2 z^2 - \omega_c z N^{-1/2} \sum_{\mathbf{k}, j} [\hat{\mathbf{B}} \times \mathbf{p}_{\mathbf{k}j}]_z. \quad (4)$$

Here, $\mathbf{p}_{\mathbf{k}j}$, $\mathbf{u}_{\mathbf{k}j}$, and $\omega_{\mathbf{k}j}$ are the 2D momentum, displacement, and frequency of the WC phonon of branch j ($j = 1, 2$) with a 2D wave vector \mathbf{k} . We chose the equilibrium in-plane position of the tunneling electron to be at the origin. Then its in-plane 2D momentum is $\mathbf{p} = N^{-1/2} \sum \mathbf{p}_{\mathbf{k}j}$ for $B = 0$.

The interaction Hamiltonian H_B (4) *does not* conserve the phonon quasi-momentum \mathbf{k} . The Hall momentum of the tunneling electron is transferred to the WC as a whole. The term H_B couples the out-of-plane motion to lattice vibrations. The problem of many-electron tunneling is thus mapped onto a familiar problem of a particle coupled to a bath of harmonic oscillators [16,9], with the coupling strength controlled by the magnetic field. The distinctions from the standard situation stem from the non-parabolicity of the potential well near the minimum and from the fact that coupled by H_B are the electron *coordinate* z and the in-plane *momenta* of the lattice. These quantities have different symmetry with respect to time inversion. In the general case [for example, where the potential energy of the system has odd-order terms in the displacements $\mathbf{u}_{\mathbf{k}j}$], the broken time-reversal symmetry requires a special approach to the analysis of tunneling [10]. The results discussed below can be appropriately generalized using this approach.

For the model (2), the analysis is simplified by the structure of the Hamiltonian (cf. [9]). For vibrations with the Hamiltonian H_v (3), one can always make a canonical transformation from the canonical coordinates and momenta $\mathbf{u}_{\mathbf{k}j}$ and $\mathbf{p}_{\mathbf{k}j}$ to the new canonical coordinates and momenta $\mathbf{p}_{\mathbf{k}j}$ and $-\mathbf{u}_{\mathbf{k}j}$, respectively. This transformation interchanges the time-reversal symmetry of the in-plane dynamical variables, it makes $\mathbf{p}_{\mathbf{k}j}$ and $\mathbf{u}_{\mathbf{k}j}$ even and odd in time, respectively. Because H_B is independent of $\mathbf{u}_{\mathbf{k}j}$ and is linear in $\mathbf{p}_{\mathbf{k}j}$, in the new variables it takes on a more familiar form of a ‘‘potential’’ coupling, with energy which depends on dynamical coordinates only and with ‘‘restored’’ time-reversal symmetry.

III. THE WKB APPROXIMATION

A. General formulation

We will evaluate the escape rate W in the WKB approximation. The major emphasis will be placed on the tunneling exponent. We will assume that the escape rate is much less than the intrawell relaxation rate for relevant states, and there is formed thermal distribution over the intrawell states of the system. This is not necessarily true for 2D systems. Our results can be generalized to the case of slow intrawell relaxation, see Sec. VII.

Electron-phonon interaction under the barrier is strong. One should therefore think of escape of the coupled electron-phonon system. It results from decay of the metastable intrawell states α , with decay rates W_α . These rates sharply increase with state energies E_α , whereas the Boltzmann intrawell distribution exponentially decreases with E_α . As a result, there is a comparatively small group of states which mostly contribute to the escape (for fast intrawell relaxation, the relative population of these states remains unchanged). This allows one to characterize escape by a single rate W ,

$$W = Z^{-1} \sum_{\alpha} W_{\alpha} \exp(-\beta E_{\alpha}), \quad (5)$$

$$W_{\alpha} = C_{\alpha} \exp[-2S_{\alpha}(\boldsymbol{\xi}_f, \boldsymbol{\xi}_{in})] |\psi_{\alpha}(\boldsymbol{\xi}_{in})|^2.$$

Here, we introduced a vector $\boldsymbol{\xi} = (z, \{\mathbf{p}_{\mathbf{k}j}\})$ with components which enumerate the z -coordinate of the tunneling electron and the ‘‘coordinates’’ $\mathbf{p}_{\mathbf{k}j}$ of the phonons, Z is the partition function calculated neglecting escape, and C_{α} are the prefactors in the partial escape rates, they will not be discussed in this paper.

The exponents in the rates W_{α} are determined [17] by the wave functions $\psi_{\alpha}(\boldsymbol{\xi})$ at the turning points $\boldsymbol{\xi}_f$ on the boundary of the classically accessible ranges ($\boldsymbol{\xi}_f$ depend on α , see below). It is convenient to evaluate $\psi_{\alpha}(\boldsymbol{\xi}_f)$ in two steps, each of which gives an exponential factor. The first factor, $\exp[-S_{\alpha}(\boldsymbol{\xi}_f, \boldsymbol{\xi}_{in})]$, describes the decay of the wave function under the barrier. Formally, it relates $\psi_{\alpha}(\boldsymbol{\xi}_f)$ to $\psi_{\alpha}(\boldsymbol{\xi}_{in})$. The point $\boldsymbol{\xi}_{in}$ is chosen close to the well, yet it lies under the barrier, so that S_{α} can be calculated in the WKB approximation. The second factor is $\psi_{\alpha}(\boldsymbol{\xi}_{in})$ itself. The resulting rate should be independent of $\boldsymbol{\xi}_{in}$.

We start with the function $S_{\alpha}(\boldsymbol{\xi}, \boldsymbol{\xi}_{in})$. To the lowest order in \hbar , for systems with time-reversal symmetry (which we ‘‘restored’’ by the canonical transformation) it is the action for a classical underbarrier motion in imaginary time $\tau = it$ with purely imaginary momenta [7]

$$p_z = i \partial S / \partial z, \quad \mathbf{u}_{\mathbf{k}j} = -i \partial S / \partial \mathbf{p}_{\mathbf{k}j}. \quad (6)$$

As a function of the imaginary time τ , the action $S(\boldsymbol{\xi}, \boldsymbol{\xi}_{in})$ is given by the integral of the Euclidean Lagrangian L_E ,

$$S_{\alpha}(\boldsymbol{\xi}, \boldsymbol{\xi}_{in}) = \int_0^{\tau} L_E d\tau - E_{\alpha} \tau, \quad (7)$$

The Lagrangian L_E is obtained from the Hamiltonian (2) using the Legendre transformation $L = p_z(dz/dt) - \sum \mathbf{u}_{\mathbf{k}j}(d\mathbf{p}_{\mathbf{k}j}/dt) - H$, followed by the transition to imaginary time, which gives

$$L_E = L_0 + L_v + L_B. \quad (8)$$

Here,

$$L_0 = \frac{m}{2} \left(\frac{dz}{d\tau} \right)^2 + U(z), \quad L_B = H_B, \quad (9)$$

and L_v is the Lagrangian of the phonons, $L_v = \sum_{\mathbf{k}j} L_{\mathbf{k}j}$, with

$$L_{\mathbf{k}j} = \frac{1}{2m} \mathbf{p}_{\mathbf{k}j} \mathbf{p}_{-\mathbf{k}j} + \frac{1}{2m\omega_{\mathbf{k}j}^2} \frac{d\mathbf{p}_{\mathbf{k}j}}{d\tau} \frac{d\mathbf{p}_{-\mathbf{k}j}}{d\tau}. \quad (10)$$

The classical equations of motion in imaginary time have the standard form

$$\frac{d}{d\tau} \frac{\partial L_E}{\partial \dot{\boldsymbol{\xi}}} - \frac{\partial L_E}{\partial \boldsymbol{\xi}} = 0. \quad (11)$$

where overdot means differentiation over τ . To calculate the escape rate, one has to find the trajectory which goes from $\boldsymbol{\xi}(0) = \boldsymbol{\xi}_{in}$ to the boundary of the classically accessible range $\boldsymbol{\xi}_f$ at a certain time τ_f and calculate the action S_{α} along this trajectory.

If the potential barrier $U(z)$ is smooth, the wave function and its derivatives under the barrier have to match the WKB wave function in the classically allowed range behind the barrier. The matching occurs at a turning point of the classical motion (11) where the derivatives of the both wave functions become equal to zero [17], i.e. for $\partial S_{\alpha} / \partial z = \partial S_{\alpha} / \partial \mathbf{p}_{\mathbf{k}j} = 0$, i.e.

$$\dot{z}(\tau_f) = 0, \quad \dot{\mathbf{p}}_{\mathbf{k}j}(\tau_f) = \mathbf{0}. \quad (12)$$

Eq. (12) is also the condition of the extremum of S_{α} with respect to the points $\boldsymbol{\xi}$ on the boundary of the classically accessible range: the escape rate is determined by the minimum of S_{α} on this boundary. A detailed analysis of the behavior of multidimensional tunneling trajectories in imaginary time for systems with time-reversal symmetry is given in Ref. [18].

Time-reversal symmetry of the equations (11) in coordinates $(z, \mathbf{p}_{\mathbf{k}j})$, together with the condition (12), show that, if the equations of motion are extended beyond τ_f , the system will bounce off the turning point and then move under the barrier back to the starting point. The section of the trajectory for $\tau > \tau_f$ is mirror-symmetrical to that for $\tau < \tau_f$,

$$z(\tau_f + \tau) = z(\tau_f - \tau), \quad \mathbf{p}_{\mathbf{k}j}(\tau_f + \tau) = \mathbf{p}_{\mathbf{k}j}(\tau_f - \tau), \quad (13)$$

where $0 \leq \tau \leq \tau_f$. As a result, the tunneling exponent $2S_\alpha$ can be calculated along the trajectory (11) that reaches the turning point at τ_f and returns to the well at $2\tau_f$.

The time τ_f is determined by the boundary conditions (12) and by the initial conditions on the trajectory, which are given by $\psi_\alpha(\boldsymbol{\xi}_{\text{in}})$. If the intrawell dynamics is semiclassical, the dominating contribution to the overall rate W (5) comes from the energies E_α for which the duration of the tunneling motion $\tau_f = \beta/2$ [7]. In the general case this is no longer true.

B. The wave function close to the well

We are interested in the case where the width of the quantum well is much less than the typical width L of the tunneling barrier. More generally, we assume that for low-lying intrawell states n , the characteristic lengths $1/\gamma_n$ of localization in the z -direction are $\gamma_n^{-1} \ll L$. Then, even where the effect of the magnetic field accumulates under the barrier and the tunneling rate is strongly changed, the field may still only weakly perturb the intrawell motion. In this case, inside the well and close to it, the out-of-plane electron motion is separated from the in-plane vibrations. Respectively, the states of the electron-phonon system can be enumerated by n and the phonon occupation numbers $n_{\mathbf{k}j}$, i.e. $\alpha = (n, \{n_{\mathbf{k}j}\})$, and the energies are

$$E_\alpha = E_n + \sum_{\mathbf{k}j} \varepsilon_{\mathbf{k}j}, \quad \varepsilon_{\mathbf{k}j} = \omega_{\mathbf{k}j} n_{\mathbf{k}j}. \quad (14)$$

Usually the interlevel distances $E_{n+1} - E_n \gg \omega_{\mathbf{k}j}$, for low-lying levels.

Because of the separation of motions, we can choose a plane $z = z_{\text{in}}$ under the barrier but close to the well, so that for $\boldsymbol{\xi} \approx \boldsymbol{\xi}_{\text{in}}$ the wave functions $\psi_\alpha(\boldsymbol{\xi})$ are semiclassical and at the same time can be factored,

$$\psi_{n, \{n_{\mathbf{k}j}\}}(\boldsymbol{\xi}) \propto e^{-\gamma_n z} \exp \left[- \sum_{\mathbf{k}j} S_{n_{\mathbf{k}j}}(\mathbf{p}_{\mathbf{k}j}) \right]. \quad (15)$$

The action $S_{n_{\mathbf{k}j}}$ determines the dependence of the wave function on the phonon coordinates.

For $\boldsymbol{\xi} = \boldsymbol{\xi}_{\text{in}}$, Eq. (15) gives the initial values of the dynamical variables $\boldsymbol{\xi}(0) \equiv \boldsymbol{\xi}_{\text{in}}$ and $\dot{\boldsymbol{\xi}}(0)$ on the WKB

trajectory (11). In particular if, for $z \approx z_{\text{in}}$, the potential $U(z)$ varies over the distance much bigger than $1/\gamma_n$, then

$$z(0) = z_{\text{in}}, \quad \dot{z}(0) = \frac{\gamma_n}{m} = \left[\frac{2[U(z_{\text{in}}) - E_n]}{m} \right]^{1/2}, \quad (16)$$

and γ_n (16) is independent of the exact position of the plane $z = z_{\text{in}}$.

It is convenient to write $S_{n_{\mathbf{k}j}}$ and $\mathbf{p}_{\mathbf{k}j}$ in Eq. (15) in the energy-phase representation, using the phonon energy $\varepsilon_{\mathbf{k}j}$ and the imaginary time $\tau_{\mathbf{k}j}$ it takes for a phonon to move under the barrier from the boundary $(2m\varepsilon_{\mathbf{k}j})^{1/2}$ of the classically allowed region to the given $\mathbf{p}_{\mathbf{k}j}$. With the Euclidean Lagrangian of the phonons (10), we have for $\mathbf{p}_{\mathbf{k}j} = [\mathbf{p}_{\mathbf{k}j}]_{\text{in}} \equiv \mathbf{p}_{\mathbf{k}j}(0)$

$$S_{n_{\mathbf{k}j}}(\mathbf{p}_{\mathbf{k}j}(0)) = \int_{-\tau_{\mathbf{k}j}}^0 d\tau L_{\mathbf{k}j}(\tau) - \varepsilon_{\mathbf{k}j} \tau_{\mathbf{k}j}, \quad (17)$$

and

$$\mathbf{p}_{\mathbf{k}j}(0) = \mathbf{e}_{\mathbf{k}j} (2m\varepsilon_{\mathbf{k}j})^{1/2} \cosh \omega_{\mathbf{k}j} \tau_{\mathbf{k}j}, \quad (18)$$

$$\dot{\mathbf{p}}_{\mathbf{k}j}(0) = \mathbf{e}_{-\mathbf{k}j} (2\varepsilon_{\mathbf{k}j} m \omega_{\mathbf{k}j}^2)^{1/2} \sinh \omega_{\mathbf{k}j} \tau_{\mathbf{k}j}$$

[$\mathbf{e}_{\mathbf{k}j}$ is the polarization vector of the mode (\mathbf{k}, j)].

C. A three-segment optimal trajectory

To evaluate the escape rate W to logarithmic accuracy, one can, following Feynman's procedure, solve the equations of motion (11) for the vibration "coordinates" $\mathbf{p}_{\mathbf{k}j}(\tau)$ in terms of $z(\tau)$ and the initial energies $\varepsilon_{\mathbf{k}j}$ and phases $\omega_{\mathbf{k}j} \tau_{\mathbf{k}j}$. Then, from the boundary condition (12), one can express $\tau_{\mathbf{k}j}$ in terms of other variables, and then perform thermal averaging by summing the escape rate over $n_{\mathbf{k}j}$ with the Boltzmann weighting factor. Here we give an alternative derivation, which provides a better insight into the structure of the tunneling trajectory.

We note that, from Eqs.(5), (7), (15), and (17), the partial escape rate W_α can be written as $W_\alpha \propto \exp(-s_\alpha)$, with

$$s_\alpha = \sum_{\mathbf{k}j} \int_{-\tau_{\mathbf{k}j}}^0 d\tau L_{\mathbf{k}j}(\tau) + \int_0^{2\tau_f} d\tau L_E(\tau) + \sum_{\mathbf{k}j} \int_{2\tau_f}^{2\tau_f + \tau_{\mathbf{k}j}} d\tau L_{\mathbf{k}j}(\tau) - 2E_n \tau_f - 2 \sum_{\mathbf{k}j} \varepsilon_{\mathbf{k}j} (\tau_f + \tau_{\mathbf{k}j}). \quad (19)$$

(the term $\gamma_n z_{\text{in}}$ in (15), which is small compared to $s_\alpha \sim \gamma_n L$, is incorporated into the prefactor, see Sec. VII A).

Eq. (19) can be interpreted in the following way: the tunneling electron in its n th state, accompanied by

phonons, move under the barrier along a classical trajectory for the imaginary time $2\tau_f$. This motion is described by the Lagrangian L_E . Before and after that, the phonons are moving on their own, disconnected from

the electronic z -motion, for times $\tau_{\mathbf{k}j}$ and with the Lagrangian L_v , so that the overall phonon trajectories make closed loops which start and end at turning points.

In the WKB approximation, the sum over the phonon occupation numbers $n_{\mathbf{k}j}$ of the weighted partial probabilities W_α (5) can be replaced by the integral over $\varepsilon_{\mathbf{k}j}$, which should then be evaluated by the steepest descent. The corrections due to the discreteness of the values of $\varepsilon_{\mathbf{k}j}$ are small provided $\omega_{\mathbf{k}j}\tau_f \ll s_\alpha$. From (19), the extremum of $\exp(-s_\alpha - \beta E_\alpha)$ with respect to $\varepsilon_{\mathbf{k}j}$ is reached for

$$\tau_{\mathbf{k}j} = \frac{1}{2}\beta - \tau_f, \quad (20)$$

This expression shows that the duration of the free phonon motion $\tau_{\mathbf{k}j}$ is the same for all vibrational modes. Moreover, the overall duration of the three-segment optimal trajectory of each vibration is $2(\tau_{\mathbf{k}j} + \tau_f) = \beta$. Examples of the trajectories are shown in Fig. 3.

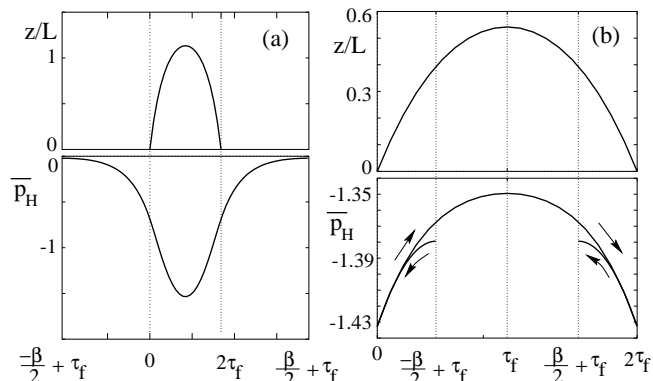


FIG. 3. Optimal trajectories of the tunneling electron $z(\tau)$ and the vibrations of the WC for $\beta > 2\tau_f$ (a) and $\beta < 2\tau_f$ (b). The numerical data refer to the Einstein model of the Wigner crystal, with $\overline{p_H}$ being the vibrational momentum in the Hall direction $\hat{z} \times \mathbf{B}$, in units $\hbar\gamma/2$. The arrows show the direction of motion along the optimal trajectory when $\beta < 2\tau_f$. The tunneling potential is of the form (30), with dimensionless cyclotron frequency $\omega_c\tau_0 = 2.0$, where $\tau_0 = 2mL/\gamma$ is the imaginary transit time for $B = 0$. The vibrational frequency is $\omega_p\tau_0 = 1.0$.

For low temperatures, $\beta > 2\tau_f$, the direction of time along the vibrational trajectory does not change, $\tau_{\mathbf{k}j} > 0$. The corresponding branch of the intrawell vibrational wave function (15) $\propto \exp(-S_{n_{\mathbf{k}j}}[\mathbf{p}_{\mathbf{k}j}(0)])$ decays with the increasing $|\mathbf{p}_{\mathbf{k}j}(0)|$ in the classically forbidden region $|\mathbf{p}_{\mathbf{k}j}(0)| > (2m\varepsilon_{\mathbf{k}j})^{1/2}$. In contrast, for $\beta < 2\tau_f$, we have $\tau_{\mathbf{k}j} < 0$. This shows that the extremum over $\varepsilon_{\mathbf{k}j}$ is reached if the intrawell vibrational wave function is analytically continued from the decaying to the increasing branch.

For $\tau_{\mathbf{k}j} = (\beta/2) - \tau_f < 0$, the “free-vibrations” term $S_{n_{\mathbf{k}j}}$ is negative, it gives rise to the decrease of the tunneling exponent. This is the formal reason why, for sufficiently high temperatures, an in-plane magnetic field

can increase the tunneling rate compared to its $B = 0$ value by coupling thermally-excited in-plane vibrations to tunneling.

If the intrawell motion transverse to the layer were semiclassical, the sum over the energy levels of this motion E_n in Eq. (5) could be replaced by an integral. The extremum of the integrand is reached for $\tau_f = \beta/2$, $\tau_{\mathbf{k}j} = 0$. This is the familiar result of the instanton theory, in which the whole system moves under the barrier from the well to the turning point and back over the imaginary time β [7]. Clearly, in this case one should not expect the tunneling rate to be enhanced by a magnetic field.

In the case of 2D electron systems, the potential well is *not* parabolic, and each term in the sum over n (5) has to be considered separately. Except for narrow parameter intervals, the contribution of one of them is dominating, and the electron tunnels from the corresponding state.

IV. THE TUNNELING EXPONENT

Eqs. (5) and (19) allow us to write the escape rate as a sum of the escape rates for different intrawell states n . To logarithmic accuracy

$$W \propto \max_n \exp(-R_n), \quad R_n = \min_{z(\tau)} \mathcal{R}_n[z(\tau)], \quad (21)$$

The functional $\mathcal{R}_n[z]$ is a retarded action functional for a 1D motion normal to the electron layer. It is determined by the functional s_α for the n th state from which the dynamical variables of the in-plane vibrations have been eliminated in a standard way [16] by solving the linear equations of motion (11) for $\mathbf{p}_{\mathbf{k}j}(\tau)$, with account taken of the expression for the duration of the phonon tunneling motion (20). This gives

$$\mathcal{R}_n[z] = \int_0^{2\tau_f} d\tau_1 \left[\frac{m}{2} \left(\frac{dz}{d\tau} \right)^2 + U(z) + \frac{1}{2} m\omega_c^2 z^2(\tau_1) \right] + \mathcal{R}_{ee}[z] + (\beta - 2\tau_f)E_n. \quad (22)$$

(we count z off from z_{in} , i.e. $z_{in} = 0$).

The term \mathcal{R}_{ee} gives the retarded action which results from the electron-electron interaction,

$$\mathcal{R}_{ee}[z] = -\frac{m\omega_c^2}{4N} \sum_{\mathbf{k}j} \omega_{\mathbf{k}j} \int_0^{2\tau_f} \int_0^{\tau_1} d\tau_1 d\tau_2 \times z(\tau_1)z(\tau_2)\chi_{\mathbf{k}j}(\tau_1 - \tau_2) \quad (23)$$

The function $\chi_{\mathbf{k}j}(\tau)$ is the phonon Green’s function,

$$\chi_{\mathbf{k}j}(\tau) = \bar{n}_{\mathbf{k}j} \exp[\omega_{\mathbf{k}j}\tau] + (\bar{n}_{\mathbf{k}j} + 1) \exp[-\omega_{\mathbf{k}j}\tau]$$

($\bar{n}_{\mathbf{k}j} = [\exp(\beta\omega_{\mathbf{k}j}) - 1]^{-1}$ is the thermal occupation number). We note that $\mathcal{R}_{ee}[z]$ can be also expressed in terms of the correlation function $\tilde{\chi}(\tau) = \langle \mathbf{p}_{\parallel}(\tau)\mathbf{p}_{\parallel}(0) \rangle$ of the

in-plane momentum \mathbf{p}_{\parallel} of an electron in the correlated 2DES,

$$\mathcal{R}_{ee}[z] = -\frac{1}{2}\omega_c^2 \int_0^{2\tau_f} \int_0^{\tau_1} d\tau_1 d\tau_2 z(\tau_1)z(\tau_2)\tilde{\chi}(\tau_1 - \tau_2). \quad (24)$$

We expect that not only does this expression apply to a Wigner crystal, but it also provides a good approximation in the case of a correlated electron liquid; it corresponds to the lowest-order term in the cumulant expansion of the appropriate propagator.

The term \mathcal{R}_{ee} is negative. It means that the electron-electron interaction in a correlated 2DES always *increases* the tunneling rate in the presence of a magnetic field. Moreover, when this term exceeds $(m\omega_c^2/2) \int z^2 d\tau$, the tunneling exponent as a whole decreases with the increasing B .

Two physical phenomena are described by the term \mathcal{R}_{ee} . One is the dynamical compensation of the Hall momentum of the tunneling electron by the WC as the electron moves under the barrier in the z -direction. The other is thermal “preparation” of the Hall momentum for the tunneling electron, which is then transformed by the magnetic field into the momentum of motion in the z -direction. We analyze these effects in the following subsections.

A. Zero temperature limit

It would be natural to think that, since tunneling is accompanied by creation of phonons for $T = 0$, then the higher the phonon frequency the lower the tunneling rate. In fact just the opposite is true.

The effect of the electron-electron interaction on tunneling, as characterized by \mathcal{R}_{ee} , depends on the interrelation between the characteristic phonon frequency ω_p and the tunneling duration τ_f . When the tunneling electron is “pushed” by the Lorentz force, it exchanges the in-plane momentum with other electrons. The parameter $\omega_p\tau_f$ determines what portion of the momentum goes to the crystal as a whole during the tunneling (note that the tunneling motion goes in imaginary time, and the quantity τ_f characterizes the time uncertainty rather than the actual duration of a real process, see Ref. [19]). As mentioned in the Introduction, in the adiabatic limit of large $\omega_p\tau_f$, all electrons have same in-plane velocity, with an accuracy to quantum fluctuations. Therefore the Lorentz force produces no acceleration, and *no phonons* are created during the tunneling. The effect of the magnetic field on tunneling should then be eliminated.

These arguments are confirmed by the analysis of Eq. (23). If the electron system is rigid enough in the plane, so that $\omega_{\mathbf{k}j}\tau_f \gg 1$, the major contribution to \mathcal{R}_{ee} comes from $\tau_1 - \tau_2 \sim \omega_{\mathbf{k}j}^{-1} \ll \tau_f$. Therefore $z(\tau_2) \approx z(\tau_1)$, so that in \mathcal{R}_{ee} the two terms $\propto \omega_c^2$ compensate each other.

The tunneling occurs as if the electron is disconnected from the phonons and does not experience a magnetic field. However, a simple analysis shows that the electron mass is effectively incremented by a B -dependent factor, and the tunneling exponent $R \equiv R_1$ is appropriately renormalized,

$$m \rightarrow m^*, \quad m^* = m \left[1 + (2N)^{-1} \sum_{\mathbf{k}j} (\omega_c^2/\omega_{\mathbf{k}j}^2) \right], \quad (25)$$

$$R = (m^*/m)^{1/2} R_{B=0}.$$

Here, the sum is limited from below by the condition $\omega_{\mathbf{k}j} > \tau_f^{-1}$; for a Wigner crystal, the dependence of the mass renormalization on the cutoff frequency is logarithmic. The tunneling rate approaches its value for $B = 0$ with increasing ω_p . On the other hand, the slope of the logarithm of the tunneling rate as a function of ω_c depends explicitly on ω_p , for $\omega_c \gtrsim \omega_p$. This provides a means for measuring ω_p .

For $\omega_p\tau_f \sim 1$, only a part of the Hall momentum can be taken by the electron crystal. The rest goes into the in-plane kinetic energy of the tunneling electron, and ultimately into creations of WC phonons. However, the major contribution to \mathcal{R}_{ee} still comes from high-frequency phonons. It can be shown from (23) that this contribution monotonically increases with increasing $\omega_{\mathbf{k}j}$. This is because the more rigid the electron system is, the more effectively it compensates the in-plane Hall momentum. An important consequence is that, since high-frequency vibrations have small wavelengths, the major effect on tunneling comes from short-range order in the electron system.

On the whole, for $T = 0$, the magnetic-field induced term in the tunneling exponent is positive, i.e. the tunneling rate decreases with the magnetic field. This can be seen from Eqs. (22), (23) by replacing $z(\tau_1)z(\tau_2)$ in \mathcal{R}_{ee} with $(1/2)[z^2(\tau_1) + z^2(\tau_2)] \geq z(\tau_1)z(\tau_2)$ and then integrating the function $\chi(\tau_1 - \tau_2) = \exp[-\omega_{\mathbf{k}j}(\tau_1 - \tau_2)]$ over τ_2 [for the term $z^2(\tau_1)$] or τ_1 [for $z^2(\tau_2)$].

Electron correlations exponentially reduce the effect of the magnetic field on the tunneling rate in a magnetic field. For specific models, the dependence of the tunneling rate on B and the vibration frequencies will be illustrated in Sec. VI, and the results will be compared with the experiment.

B. Small phonon frequencies

The analysis of the tunneling rate somewhat simplifies in the case of comparatively high temperatures and small phonon frequencies, where the vibrations are classical and their frequencies are small compared to the reciprocal tunneling duration, $\omega_{\mathbf{k}j}\beta, \omega_{\mathbf{k}j}\tau_f \ll 1$. In this case

$$\mathcal{R}_{ee}[z] = -2mT\omega_c^2\tau_f^2\bar{z}^2, \quad \bar{z} = \tau_f^{-1} \int_0^{\tau_f} d\tau z(\tau) \quad (26)$$

[since we chose $z_{\text{in}} = 0$ and $z_f > 0$, we have $\mathcal{R}_{\text{ee}} < 0$ in Eq. (26)].

Eqs. (22), (26) describe also the tunneling action of a single electron, with the Maxwell distribution of the in-plane momentum inside the well $\exp(-p^2/2mT)$. The coupling of the $\hat{\mathbf{z}} \times \mathbf{B}$ component of the momentum to the out-of-plane motion gives rise to the term $-2p\omega_c \int_0^{\tau_f} d\tau z(\tau)$ in the tunneling action [cf. Eqs. (4), (7)]. The extreme value of the sum of this term and $-p^2/2mT$ is just equal to $-\mathcal{R}_{\text{ee}}[z]$ as given by (26).

The single-electron form of the tunneling exponent is to be expected in the limit of small $\omega_{\mathbf{k}j}$, because the distribution over in-plane momenta of electrons forming a Wigner crystal is Maxwellian, in the classical limit. For small $\omega_{\mathbf{k}j}\tau_f$ the momenta do not change over the tunneling duration, therefore only the momentum of the tunneling electron itself is important. The above derivation provides an independent test of the derivation used to obtain the general expression (22), (23).

We note that the action $\mathcal{R}_{\text{ee}}[z]$ (26) is still retarded, it does not correspond to a local in time Lagrangian. The functional form of \mathcal{R}_{ee} remains the same even for temperatures $T \lesssim \omega_{\mathbf{k}j}$ provided the phonon frequencies are small compared to τ_f^{-1} and ω_c . In this case T in Eq. (26) has to be replaced by $(4N)^{-1} \sum \omega_{\mathbf{k}j}(2\bar{n}_{\mathbf{k}j} + 1)$. This factor explicitly depends on the phonon dispersion law, but again, the major contribution comes from short-wavelength high-frequency phonons, which are determined by the short-range order in the electron system.

V. ENHANCEMENT OF TUNNELING BY A MAGNETIC FIELD

In this section we describe a new effect, the enhancement of the tunneling rate by a magnetic field parallel to the electron layer. Qualitatively, the enhancement is due to transferring the energy of thermal in-plane motion into the energy of out-of-plane tunneling. On the formal level it is a consequence of the increase, with increasing temperature, of the absolute value of the term \mathcal{R}_{ee} (23) in the tunneling action. Since this term gives a negative contribution to the tunneling exponent R , the whole B -dependent term in \mathcal{R} becomes negative starting with a certain crossover temperature T_c , and then the tunneling rate increases with B . The range boundaries where the overall escape rate increases with B are not universal and depend on the potential $U(z)$ and the phonon spectrum. The enhancement occurs in a limited temperature range, and may start from $B = 0$ or have a finite threshold in B . However, very strong fields suppress rather than enhance escape.

A. The crossover temperature

The lower temperature bound of the enhancement domain is the crossover temperature T_c . It can be determined from the small- B expansion of the tunneling exponent for the ground state [$n = g$ in Eq. (21)],

$$R_g(\omega_c) \approx R_g(0) + A_g(T)\omega_c^2, \quad \omega_c\tau_0 \ll 1 \quad (27)$$

where τ_0 is the tunneling time in the ground state for $B = 0$. The role of the ground state is special in that the barrier width is bigger for the ground state energy than for the energies of the excited states. Therefore the effect of the magnetic field, which accumulates under the barrier, is most pronounced in the ground state.

The value of A_g is given by the terms $\propto \omega_c^2$ in the action R_g (22) calculated along the tunneling trajectory $z_0(\tau)$ for $B = 0$. From the analysis in Sec. IV A it follows that $A_g > 0$ for $T \rightarrow 0$. The crossover temperature is given by

$$A_g(T_c) = 0. \quad (28)$$

For $T > T_c$ the tunneling exponent R_g decreases and the tunneling rate increases with B , for small B .

In the limit of low phonon frequencies, $\omega_{\mathbf{k}j} \ll 1/\tau_0, T_c$, from Eqs. (22), (26) it follows that $\beta_c \equiv 1/T_c = 2\tau_0 \bar{z}_0^2 / \bar{z}_0^2$, where \bar{z}_0 is the average coordinate \bar{z} (26) for the $B = 0$ trajectory with energy E_g , and \bar{z}_0^2 is the mean square value of z on the same trajectory,

$$\bar{z}_0^2 = \tau_0^{-1} \int_0^{\tau_0} d\tau z_0^2(\tau) \quad (E = E_g).$$

Clearly, in this case $\beta_c < 2\tau_0$. It follows from Eq. (23) that $2\tau_0$ is also the limiting value of β_c in the opposite case of high phonon frequencies, $\omega_{\mathbf{k}j} \gg 1/\tau_0$. On the whole, we have the bounds on temperature for the tunneling enhancement in the ground intrawell state

$$2\tau_0 \frac{\bar{z}_0^2}{z_0^2} < \beta_c < 2\tau_0. \quad (29)$$

As noted above, \bar{z}_0 is nonzero, and generally $\bar{z}_0^2/z_0^2 \sim 1$.

It follows from the above arguments that the value of the crossover temperature $T_c = 1/\beta_c$ decreases with increasing phonon frequencies, that is the crossover is determined by high-frequency phonons which, in the case of 2D electron systems, have large wave numbers and are determined by the short-range order.

B. Upper temperature limit

A thresholdless tunneling enhancement starting from $B = 0$, occurs for temperatures bounded from above by the condition that the system tunnels from the ground state rather than from excited intrawell states or via thermal activation over the barrier. In principle, even for excited states, the tunneling rate may increase with B , but

this does not happen for simple model potentials investigated below.

If the tunneling is enhanced only in the ground state, the upper temperature bound is often the temperature $T_{1\rightarrow 2}$ where the probability of tunneling from the first excited state, weighted with the occupation factor, exceeds that from the ground state, for $B = 0$. It can be estimated for smooth tunneling barriers, where the tunneling duration $\tau_0(E)$ for $B = 0$ often decreases with the increasing energy E . In fact, the function $\tau_0(E)$ may be nonmonotonic even for simple potentials $U(z)$; a detailed analysis of this function lies outside the scope of this paper, but generalization of the results to appropriate cases is straightforward. From (22), for decreasing $\tau_0(E)$, switching from tunneling from the ground state ($n = 1$) to that from the first excited state ($n = 2$) occurs for the reciprocal temperature

$$\beta_{1\rightarrow 2} = 2 \frac{\int_{E_1}^{E_2} \tau_0(E) dE}{E_2 - E_1} \quad (E_1 \equiv E_g).$$

This value lies between $2\tau_0(E_2)$ and $2\tau_0(E_1)$. Depending on the tunneling potential, $\beta_{1\rightarrow 2}$ can be smaller or larger than β_c (29). If a magnetic field does not increase the rate of tunneling from the state $n = 2$, thresholdless tunneling enhancement occurs for $T_c < T_{1\rightarrow 2}$.

Alternatively, for $B = 0$ the system may switch to activated escape over the barrier with increasing temperature for $T = T_a < T_c$. The thresholdless tunneling enhancement by the magnetic field does not occur in this case. However, in this as well as in the previous case there may still occur a B -induced enhancement of the escape rate, starting with some nonzero B . We note that in the above arguments, it was assumed that thermalization inside the well is faster than electron escapes.

C. Field-induced switching between the levels and from activation to tunneling

Even in the temperature range $T > T_{1\rightarrow 2}$ a sufficiently strong magnetic field can increase the tunneling rate, provided $T > T_c$. This happens if the tunneling exponent for the ground state $R_g(\omega_c) \equiv R_{n=1}(\omega_c)$ exceeds that in the first excited state $R_{n=2}(\omega_c)$ and its zero-field value $R_{n=2}(0)$. In a certain temperature range where $T > T_{1\rightarrow 2}$, the tunneling rate for $B = 0$ is determined by tunneling from the excited state $n = 2$. This rate decreases with increasing B (the tunneling exponent $R_{n=2}$ increases with B). For some B the exponents $R_{n=2}(\omega_c)$ and $R_{n=1}(\omega_c)$ become equal to each other. For larger B the system tunnels from the ground state, and the tunneling rate increases with B .

Similarly, since the activation rate is only weakly affected by B , in a certain temperature range where escape already occurs via activation for $B = 0$, starting

with some B it may again go through tunneling from the ground state. This happens if the tunneling rate for the ground state becomes bigger than the activation rate and only happens in a limited range of B , see Sec. VI. For a special model the switching is illustrated in Fig. 6 below.

VI. TUNNELING ENHANCEMENT FOR THE EINSTEIN MODEL OF A WIGNER CRYSTAL

In what follows we will illustrate the general results and apply them to specific 2D systems assuming that all vibrational modes have the same frequency, $\omega_{\mathbf{k}j} = \omega_p$, i.e. using the Einstein model of the Wigner crystal. This is motivated by the fact that the tunneling is determined primarily by short-wavelength vibrations, which have a comparatively weak dispersion. Correspondingly, when we discuss the experiment, we will set ω_p equal to the characteristic short-wavelength plasma frequency $(2\pi e^2 n^{3/2}/m)^{1/2}$, where n is the electron density.

A. Triangular barrier

For electrons above helium surface and in certain types of semiconductor heterostructures, the potential $U(z)$ in the barrier region ($z \geq 0$) is determined by the electric field which pulls electrons away from the intrawell states. To a good approximation $U(z)$ is then linear in z ,

$$U(z) = \frac{\gamma^2}{2m} \left(1 - \frac{z}{L}\right) \quad (z \geq 0). \quad (30)$$

Here, $\gamma \equiv \gamma_1$ is the decrement of the ground-state wave function $\psi_g \equiv \psi_1$ near the well, $\partial \ln \psi_1 / \partial z = -\gamma$ for $z = 0$, cf. the discussion before Eq. (16). The additive constant in $U(z)$ is chosen so that the energy of the ground state $E_g = 0$. Then L is the tunneling length in the ground state for $B = 0$. It is determined by the pulling electric field. We assume that $\gamma L \gg 1$.

The approximation (30) applies only within the barrier region, where U is determined by the pulling electric field, and not inside the well, where $U(z)$ is singular. Moreover, it holds provided the width of the tunneling barrier is small compared to the in-plane interelectron distance $n^{-1/2}$ [cf. Eq. (38) below].

In order to calculate the ground-state tunneling exponent, it is convenient to solve directly the equations of motion (11) with the boundary conditions (16), (18), (12), and (20). For a triangular potential, these equations are linear. This allowed us to obtain for the tunneling exponent a simple expression

$$\begin{aligned} \tilde{R} = & -\nu_p^2 \tau_{\text{red}}^3 + 3\nu_p \tau_{\text{red}} (1 - \tau_{\text{red}}) \coth[\omega_p \beta / 2 - \nu_p \tau_{\text{red}}] \\ & + 3 + 3\tau_{\text{red}} (\nu^2 - 1), \quad R_g = 2\gamma L \tilde{R} / 3\nu^2. \end{aligned} \quad (31)$$

Here, $\nu_p = \omega_p \tau_0$ and $\nu_c = \omega_c \tau_0$ are the dimensionless in-plane and cyclotron frequencies scaled by the tunneling duration τ_0 for $B = 0$, and $\nu^2 = \nu_p^2 + \nu_c^2$.

The quantity $\tau_{\text{red}} = \tau_f / \tau_0$ in Eq. (31) is the reduced tunneling duration. It is given by the equation

$$\begin{aligned} & [(1 - \tau_{\text{red}})\nu_p \nu^2 \coth[\omega_p \beta / 2 - \nu_p \tau_{\text{red}}] - \nu_c^2] \tanh \nu \tau_{\text{red}} \\ &= \nu [\nu_p^2 \tau_{\text{red}} - \nu^2] \end{aligned} \quad (32)$$

In the limit $T \rightarrow 0$, Eqs. (31), (32) go over into the result obtained earlier [10] (in Ref. [10] we used ω_0 and ν_0 instead of ω_p and ν_p , respectively). In this limit, the role of the many-electron effects is particularly important. In the single-electron approximation ($\omega_p = 0$) the tunneling duration τ_f and the tunneling exponent R_g diverge for $\omega_c \rightarrow \tau_0^{-1}$ [5]. This happens because the effective single-electron potential $U(z) + (1/2)m\omega_c^2 z^2$, which takes into account the parabolic magnetic barrier, does not have classically allowed extended states with energy $E_g = 0$ behind the barrier.

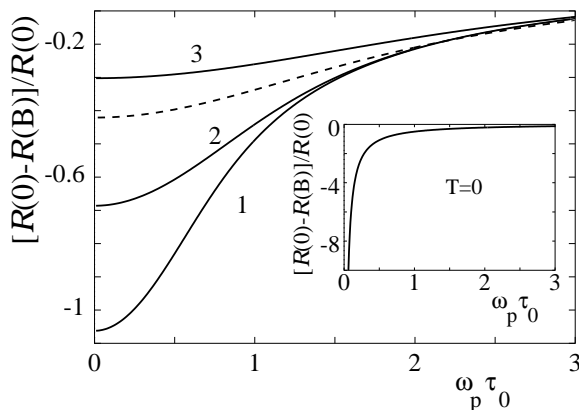


FIG. 4. The tunneling exponent in the ground state for a triangular potential barrier (30) as a function of the phonon frequency ω_p in the Einstein model of the Wigner crystal for $\omega_c \tau_0 = 2$. The time $\tau_0 = mL/\gamma$ is the duration of tunneling for $B = 0$ and $T = 0$. The curves 1 to 3 refer to reciprocal temperatures $\beta/\tau_0 = 7, 5, 3$. The dashed line is the result of the direct variational method, with one variational parameter τ_f .

The inter-electron momentum exchange makes tunneling possible for all B . For $\omega_c \tau_0 > 1$ and $T = 0$, the tunneling exponent is a step function of the exchange rate ω_p in the limit of slow exchange, $\omega_p \tau_0 \ll 1$. In the opposite limit of the fast momentum exchange, $\omega_p \gg \tau_0^{-1}$, ω_c , from Eqs. (31), (32) we obtain $\tau_{\text{red}} \approx 1$ [i.e., $\tau_f \approx \tau_0$], and $R_g \approx 4\gamma L/3$. These are the values for tunneling for $B = 0$. The overall dependence of the tunneling exponent on ω_p for $T = 0$ is shown in the inset of Fig. 4.

For a given magnetic field, the dependence of the tunneling exponent R_g on the frequency ω_p becomes much less steep with increasing temperature, as seen from Fig. 4. For large $\omega_p \tau_0$, $\omega_p \beta$, the curves for different

temperatures merge together and approach the $B = 0$ asymptote.

The value of R_g can be calculated independently from the functional \mathcal{R}_n (22) using the direct variational method. Even a simple approximation where $z(\tau)$ is quadratic in τ , with the only variational parameter being the tunneling duration τ_f , gives a reasonably good result, which is shown in Fig. 4 by a dashed line for $\beta = 3\tau_0$. Such calculation gives a good approximation for higher temperatures, and also for lower temperatures but not too small $\omega_0 \tau_0$. For low temperatures and small $\omega_0 \tau_0$ the trajectory $z(\tau)$ is strongly nonparabolic, and more than one parameter is required in the variational calculation.

B. Field-induced tunneling enhancement and switching to tunneling from activation

The explicit expression for the tunneling exponent (31) allows us to analyze the effects of tunneling enhancement and magnetic field induced switching to tunneling, which were discussed in Sec. V. In the small- B limit, where $\omega_c \ll \omega_p, \tau_0^{-1}$, the tunneling exponent $R_g(B)$ is seen from Eq. (31) to be quadratic in B . The coefficient A_g in Eq. (27) can be easily calculated. From the condition $A_g = 0$ we obtain the value of the reciprocal temperature β_c which corresponds to the crossover from decrease to increase of the tunneling rate due to a magnetic field,

$$\beta_c = 2\tau_0 + \frac{2}{\omega_p} \tanh^{-1} \left[\frac{\nu_p [3\nu_p - (3 + \nu_p^2) \tanh \nu_p]}{\nu_p^3 - 3\nu_p + 3 \tanh \nu_p} \right]. \quad (33)$$

In agreement with (29), β_c monotonically increases with ω_p from $5\tau_0/3$ at $\omega_p = 0$ to $2\tau_0$ for $\omega_p \rightarrow \infty$.

The dependence of the tunneling exponent (31) on the magnetic field for different temperatures is shown in Fig. 5. Above the crossover temperature ($\beta < \beta_c$), $R(B)$ decreases, and $R(0) - R(B)$ and the tunneling probability increase with the increasing field, for small B . The slope $dR/BdB \propto \beta - \beta_c$ for $B \rightarrow 0$. However, for strong fields the tunneling rate decreases with the increasing B , because the Hall momentum can no longer be compensated by thermal fluctuations. For small $\omega_p \tau_0$ this happens when the typical Hall momentum $m\omega_c L$ becomes comparable to the thermal momentum $(2mT)^{1/2}$ multiplied by the small factor $(\gamma L)^{-1/2}$. This factor comes from the fact that the optimal value of the transferred in-plane momentum in the single-electron approximation is determined by the maximum of the sum $2S_E[p] + (p^2/2mT)$, where $S_E[p] \propto \gamma L$ is the single-electron action in the magnetic field for given in-plane momentum p . Therefore the thermal momentum is scaled by $(\gamma L)^{1/2}$.

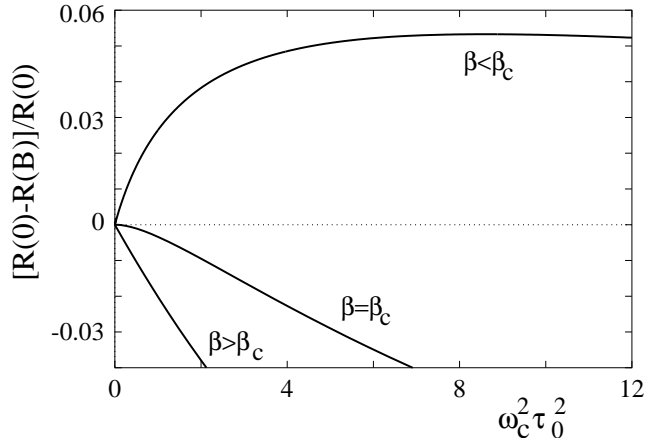


FIG. 5. The dependence of the tunneling exponent $R(B) \equiv R_g(B)$ on the magnetic field (31) for $\omega_p \tau_0 = 1/3$ near the crossover temperature $\beta_c \approx 1.67\tau_0$ (33). The curves 1 to 3 correspond to $(\beta - \beta_c)/\tau_0 = 0.2, 0, -0.3$

It is clear from the data in Fig. 5 that, for the barrier chosen, the magnetic field induced increase of the tunneling exponent R is numerically small. However, for typical $R \gtrsim 50$ it can still be noticeable, although strictly speaking it is on the border of applicability of the approximation in which only the exponent is taken into account.

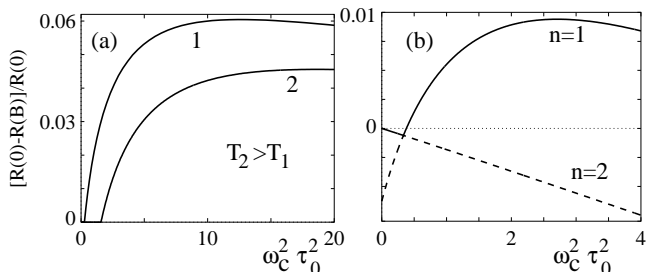


FIG. 6. Magnetic field induced switching from activation (a) and from tunneling from the excited state (b) to tunneling from the ground state, for $\omega_p \tau_0 = 1/3$. In (a), there is only one intrawell state in the potential well $U(z)$, and the transition to activation for $B = 0$ occurs for $\beta/\tau_0 = 4/3$. The curves 1, 2 correspond to $(\beta - \beta_c)/\tau_0 = -0.35, -0.4$. In (b), the position E_2 of the excited level ($n = 2$) is chosen at $0.2\gamma^2/2m$ below the barrier top ($E_1 = 0$). The temperature is chosen at $(\beta - \beta_c)/\tau_0 = -0.16$, so that for $B = 0$ the system tunnels from the excited state. The observable (smaller) tunneling exponents for a given B are shown with bold lines, whereas dashed lines show the bigger exponents, which correspond to smaller tunneling rates.

The expression (31) gives the tunneling exponent only for low enough temperatures where the system escapes from the ground state. For higher temperatures, one should take into account the possibility of escape from excited states and via an activated transition over a potential barrier. The positions of the excited levels depend not only on the barrier shape, but also on the shape of

the potential $U(z)$ inside the well. The analysis for a realistic system, electrons on the surface of liquid helium, is done in the next section. Here, in order to illustrate different options, we discuss two cases: a narrow well, in which case the ground state is essentially the only intrawell state, and a well with a comparatively shallow excited state. We assume that the intrawell relaxation rate is higher than the escape rate.

We start with the case of one bound state in the potential well. For $B = 0$ and a triangular barrier $U(z)$ (30), switching from tunneling to activation occurs here for the temperature $T_a \equiv 1/\beta_a = (4\tau_0/3)^{-1}$. This temperature is higher than the crossover temperature $1/\beta_c$ (33), and therefore there is a region where the enhancement of tunneling by a magnetic field can be observed, as discussed above (cf. Fig. 5). However, even though for $T > T_a$ the $B = 0$ -escape occurs via overbarrier transitions, the increase of the tunneling rate with the increasing B can make tunneling more probable for sufficiently strong B . If the activation rate is independent of B , the overall dependence of the exponent of the escape rate $R(B)$ on B is shown in Fig. 6a. In this case, $R(0) = \gamma^2/2mT$ is the barrier height over temperature. Switching to tunneling and to the increase of the escape rate with B occurs where the tunneling exponent $R_g(B)$ as given by Eq. (31) becomes less than $R(0)$.

A similar switching occurs in the temperature range where tunneling from the first excited level is more probable than from the ground state, for $B = 0$. Since with increasing B the tunneling rate in the ground state increases, the system switches to tunneling from the ground state starting with a certain value of B . This is illustrated in Fig. 6b.

In narrow-well potentials, a magnetic field may strongly affect the wave functions with energies close to the barrier top. As a result, new bound metastable states may appear in a strong field. The field also shifts the energy levels of the existing states. The rate of inter-level transitions may also change, since the field mixes together the in-plane and out-of-plane motions. The related effects may become important with increasing temperature.

C. Square barrier: field-induced crossover to thermal activation

In many physically interesting systems, the tunneling barrier $U(z)$ is nearly rectangular. This is often the case for semiconductor heterostructures, where the barrier is formed by the insulating layer. If we count U off from the intrawell energy level E_g and set the boundaries at $z = 0$ and $z = L$, the barrier has the form

$$U(z) = \gamma^2/2m, \quad 0 < z < L. \quad (34)$$

Here, $1/\gamma$ is the decay length under the barrier, cf. Eq. (16), and we have neglected the lowering of the barrier due to the electrostatic field from other electrons at their lattice sites, which is a good approximation for $nL^2 \ll 1$.

We assume that, behind the barrier ($z > L$), an electron can move semiclassically with all energies. Then the decaying underbarrier wave function has to be matched to an appropriate propagating wave behind the barrier at $z = L$. In contrast to the case of a smooth barrier, because the potential $U(z)$ is discontinuous at $z = L$, the z -component of the momentum should not be the same on the opposite sides of the boundary. However, the in-plane ‘‘momentum’’ components $\mathbf{u}_{\mathbf{k}j}$, which are imaginary under the barrier, still have to be continuous. Respectively, the boundary conditions (12) for the tunneling trajectory should be changed to

$$z(\tau_f) = L, \quad \mathbf{u}_{\mathbf{k}j}(\tau_f) = \mathbf{0}. \quad (35)$$

In fact, the condition $\mathbf{u}_{\mathbf{k}j} = \mathbf{0}$ gives the in-plane values of $\mathbf{p}_{\mathbf{k}j}$ for which the wave function is maximal for $z = L$.

With the boundary conditions (35), elimination of phonon variables from the Euclidean action S_E in the tunneling exponent is similar to what was done for a smooth barrier. The resulting expression for the retarded functional $\mathcal{R}_n[z]$ coincides with Eq. (22), provided $z(\tau_f + x)$ is defined as $z(\tau_f - x)$, for $0 \leq x \leq \tau_f$.

An important feature of a rectangular tunneling barrier is that the tunneling time $\tau_0(E) = -dS_0/dE$ for $B = 0$ monotonically increases with energy E . Therefore the maximum of the function $-\beta E - 2S_0(E)$, which gives the probability of tunneling with energy E with account taken of the occupation factor, corresponds either to the transition from the ground state or to activation over the barrier. Switching to activation occurs for the temperature $T_a = \gamma^2/4mS_0(E_g) \equiv \gamma/4mL = (4\tau_0)^{-1}$. It is lower than the temperature T_c of the crossover from B -suppressed to B -enhanced tunneling as given by Eq. (29), and therefore we do not expect the crossover to occur in systems with a square barrier.

If the temperature $T < T_a$, escape for $B = 0$ occurs via tunneling, and its probability decreases with the in-

creasing B . Starting with some B , where the tunneling exponent becomes bigger than the activation exponent $\gamma^2/2mT$, it becomes more probable to escape by activated transition than by tunneling. To a good approximation, the escape rate becomes then independent of the magnetic field.

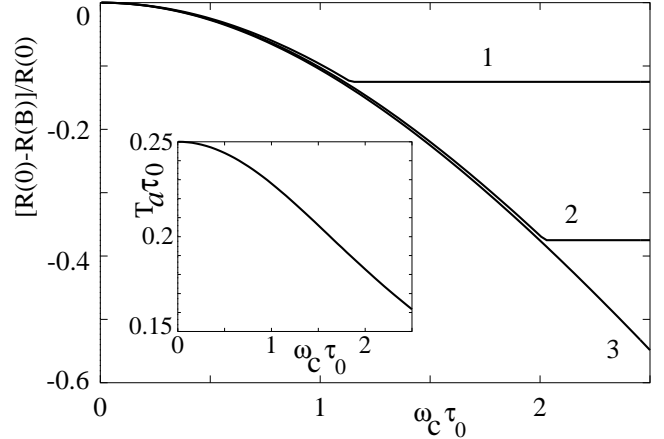


FIG. 7. The logarithm of the escape rate $R(B)$ for the square potential barrier, $\omega_p = (2\tau_0)^{-1}$ ($\tau_0 = mL/\gamma$). The value $R(0)$ is given by the tunneling exponent, $R(0) = 2S_0(E_g) \equiv 2\gamma L$. Curves 1 to 3 correspond to $\beta/\tau_0 = 4.5, 5.5, 6.5$. The sections of the curves where $R(B)$ increases correspond to tunneling and are described by Eq. (36), whereas the horizontal sections of the curves correspond to thermal activation. Inset: the magnetic field dependence of the switching temperature $T_a\tau_0$.

The B -dependence of the escape rate for different temperatures is illustrated in Fig. 7. The results refer to the Einstein model of the Wigner crystal. In this model the tunneling exponent can be obtained directly from the [linear, in this case] equations of motion (11) with the boundary conditions (16), (18), (35). It has the form

$$R_g = \gamma L [1 + \tau_{\text{red}} + \nu_c \kappa(\tau_{\text{red}})], \quad (36)$$

where the function $\kappa(\tau_{\text{red}})$ and the reduced tunneling time $\tau_{\text{red}} = \tau_f/\tau_0$ are given by the equations

$$\begin{aligned} \kappa(\tau_{\text{red}}) &\equiv \frac{\nu_c (\cosh \nu \tau_{\text{red}} - 1)}{\nu_c^2 + \nu_p^2 \cosh \nu \tau_{\text{red}} + \nu \nu_p \coth[\omega_p \beta / 2 - \nu_p \tau_{\text{red}}] \sinh \nu \tau_{\text{red}}} \\ &= \frac{1}{\nu_c \nu_p^2} \frac{\nu_c^2 (2 - 2 \cosh \nu \tau_{\text{rd}} + \nu \tau_{\text{rd}} \sinh \nu \tau_{\text{rd}}) - \nu^3 (\tau_{\text{rd}} - 1) \sinh \nu \tau_{\text{rd}}}{(1 - \cosh \nu \tau_{\text{rd}})(1 - \nu_c^2/\nu_p^2) + \nu \tau_{\text{rd}} \sinh \nu \tau_{\text{rd}}} \end{aligned} \quad (37)$$

with $\nu_p = \omega_p \tau_0$, $\nu_c = \omega_c \tau_0$, and $\nu = (\nu_p^2 + \nu_c^2)^{1/2}$.

The temperature of switching to activation is given by the equation $T_a = \gamma^2/2mR_g$. From (36), (37), both R_g and the reduced time τ_{red} increase with the mag-

netic field, and therefore the switching temperature T_a decreases with B . However, it follows from the analysis of the above equations that T_a remains lower than $1/(2\tau_f)$, and $\tau_f \geq \tau_0$ for all temperatures where the sys-

tem escapes via tunneling, in contrast to the case of the triangular barrier discussed earlier.

The effect of saturation of the escape rate with increasing B is not limited to square barriers, of course. For strong enough B and nonzero temperatures, the tunneling rate becomes less than the activation rate, and the system switches to activation; the switching may go in steps with increasing B , via tunneling from excited intrawell states.

VII. COMPARISON WITH THE EXPERIMENTAL DATA ON TUNNELING FROM HELIUM SURFACE

Tunneling from a strongly correlated 2DES has been investigated in much detail for electrons on helium surface [20,5]. In this system, a good agreement has been reached between theory and experiment in the absence of the magnetic field, where the primary role of the electron correlations is to change the effective single-electron tunneling barrier (see below). As mentioned before, there were also done interesting experiments on tunneling in a magnetic field. However, the observed strong field dependence of the tunneling rate dramatically differed from the predictions of the single-electron theory and has remained unexplained [5].

Electrons on helium surface are localized in a 1D potential box. One side of this box is the image potential $-\Lambda/z$, where $\Lambda = e^2(\epsilon - 1)/4(\epsilon + 1)$ ($\epsilon \approx 1.057$ is the dielectric constant of helium), and z is the direction normal to the surface. The other side is a high barrier ~ 1 eV on the surface ($z = 0$), which prevents electrons from penetrating into the helium. The intrawell states can be made metastable by applying a field \mathcal{E}_\perp which pulls the electrons away from the surface. This field is determined by the helium cell geometry and depends on the applied voltage and the electron density n , cf. [21]. The overall electron potential has the form

$$U(z) = -\Lambda z^{-1} - |e\mathcal{E}_\perp|z - m\bar{\omega}^2 z^2 \quad (z > 0). \quad (38)$$

The term $\propto \bar{\omega}^2$ describes the Coulomb field created by other electrons at their in-plane lattice sites (the ‘‘correlation hole’’ [15,22]). Only the lowest-order term in the ratio of the tunneling length L to the interelectron distance $n^{-1/2}$ has been kept in Eq. (38), and we used the interrelation

$$\bar{\omega} = \left[\frac{e^2}{2m} \sum_l' |\mathbf{R}_l|^{-3} \right]^{1/2} \equiv \left[\frac{1}{2N} \sum_{\mathbf{k}j} \omega_{\mathbf{k}j}^2 \right]^{1/2} \quad (39)$$

for the sum over lattice sites \mathbf{R}_l . For a triangular lattice, $\bar{\omega} \approx (4.45e^2n^{3/2}/m)^{1/2}$ [23]. The conditions $1/\gamma \ll L \ll n^{-1/2}$ are typically very well satisfied in experiment, with the decay length $1/\gamma = 1/\Lambda m \approx$

0.7×10^{-6} cm, $L \sim |E_g/e\mathcal{E}_\perp| \approx \gamma^2/2m|e\mathcal{E}_\perp| \sim 10^{-5}$ cm, and $n^{-1/2} \sim 10^{-4}$ cm [in the estimate of L we used that $|E_g| \gg |e\mathcal{E}_\perp|/\gamma$, $m\bar{\omega}^2/\gamma^2$, and that $|e\mathcal{E}_\perp|/\gamma \gtrsim \bar{\omega}$].

To compare the predicted dynamical effect of the electron-electron interaction with the experimental data on tunneling in the magnetic field [5], we use the Einstein model of the WC. In the equations of motion (11) we assume that all phonon frequencies $\omega_{\mathbf{k}j}$ are the same and set them equal to the characteristic plasma frequency $\omega_p = (2\pi e^2 n^{3/2}/m)^{1/2}$ [yet we use Eq. (39) for the parameter $\bar{\omega}$ of the potential barrier $U(z)$]. The numerical results change only slightly when the phonon frequency is varied within reasonable limits, e.g., is replaced by $\bar{\omega}$.

The magnetic field dependence of the tunneling rate for the parameters used in the experiment is calculated from Eqs. (11), (16), (12), (18) and is shown in Fig. 8. The data refer to the values of T where escape occurs via tunneling from the ground state. The actual calculation is largely simplified by the fact that, deep under the barrier, the image potential $-\Lambda/z$ in (38) can be neglected. The equations of motion (11) become then linear, and the tunneling exponent R can be obtained in an explicit, although cumbersome form, which was used in Fig. 8. The correction to R from the image potential is $\sim 1/\gamma L$, which is the small parameter of the theory. Moreover, since this correction comes from the range of small z , where the effect of the magnetic field is small, it is largely compensated where $R(B) - R(0)$ is calculated. This and other corrections $\sim 1/\gamma L$ result in changes of the theoretical curves that are smaller than the uncertainty in $R(B) - R(0)$ due to the uncertainties in n and \mathcal{E}_\perp in the experiment [5].

As seen from Fig. 8, the dynamical many-electron theory is in good qualitative and quantitative agreement with the experiment, without any adjustable parameters. At low temperatures ($T = 0.04$ K), the many-electron tunneling rate is bigger than the single-electron estimate [5] by a factor of 10^2 for $B = 0.25$ T. For this temperature, the tunneling rate is well described by the $T \rightarrow 0$ limit [29]. The B -dependence of the tunneling rate is very sensitive to temperature. It becomes less pronounced for higher T , and the role of dynamical many-electron effects becomes less important, too. Interestingly, the theoretical data on the *ratio* of $W(B)/W(0)$ become less sensitive to the experimental uncertainties in the cell geometry (which determines \mathcal{E}_\perp) and the electron density n for intermediate temperatures $T \sim 0.14$ K. This is because the corresponding errors in $W(B)$ and $W(0)$ compensate each other for such temperatures.

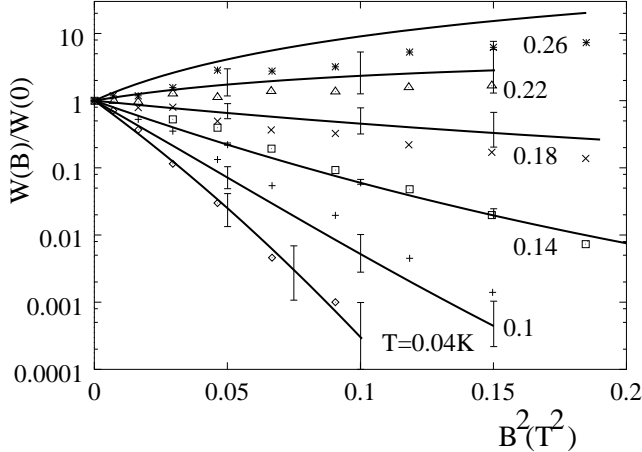


FIG. 8. The relative rate of electron tunneling from the helium surface $W(B)/W(0)$ as a function of the magnetic field B for the electron density $n = 0.8 \times 10^8 \text{ cm}^{-2}$ and the calculated pulling field $\mathcal{E}_\perp = 24.7 \text{ V/cm}$ (solid curve). Solid lines show how the theory compares to the experimental data points of Ref. [5]. The error bars show the uncertainty in the theoretical values due to the uncertainty in the parameters of the experiment.

The crossover to magnetic-field enhanced tunneling occurs for temperature $T_c \approx 0.19 \text{ K}$, for the parameters in Fig. 8. The expected increase of the tunneling rate with B for $T > T_c$ is shown in Fig. 8. It has indeed been observed in the experiment [5]. The analysis of the experiment requires to establish whether, for temperatures of interest, escape actually occurs via tunneling. To that end we note first that, as it follows from a direct variational calculation, the potential $U(z)$ (38), with the parameter values specified in Fig. 8, has only one metastable intrawell state.

If the intrawell relaxation were fast enough, the temperature of the crossover from tunneling to activation T_a for $B = 0$ would be given by the condition that the tunneling exponent R_g be equal to the activation exponent $(U_{\max} - E_g)/T$ [here, U_{\max} is the maximal value of the potential $U(z)$]. This would give $T_a \approx 0.15 \text{ K}$. However, activated escape requires that the in-plane thermal energy of an electron be transformed into the energy of its out-of-plane motion. This involves a large transfer of the in-plane momentum $\sim [2m(U_{\max} - E_g)]^{1/2}$. The electron-electron interaction does not give rise to such a transfer in a strongly correlated system, since the reciprocal interelectron distance is $n^{1/2} \ll [2m(U_{\max} - E_g)]^{1/2}$.

The major process which gives rise to the momentum transfer is scattering by capillary waves on the helium surface, ripplons [2]. Electron-ripplon coupling is weak. As a result, the prefactor in the activation rate, which is quadratic in the coupling constant, is small. For $B = 0$ it is $\sim \gamma^2 T^2 / \hbar \sigma$ [24], where σ is the surface tension of liquid helium. For temperatures $T < 0.25 \text{ K}$ this prefactor is less than the prefactor in the tunneling rate $(\hbar \gamma^2 / m) \exp(-2)$ by a factor $< 10^{-5}$. Therefore the

crossover from tunneling to activation occurs for higher temperatures than it would follow from the condition of equal tunneling and activation exponents.

For the parameters in Fig. 8, the rates of activation and tunneling escape become equal for temperatures slightly higher than 0.26 K (for $B = 0$). Therefore the experimentally observed increase of the escape rate with B is indeed due to the discussed mechanism of B -enhanced tunneling. The smaller experimental values of the relative escape rate $W(B)/W(0)$ for $T = 0.26 \text{ K}$ can be understood by noticing that the activation rate is close to the tunneling rate for such T , and since it presumably only weakly depends on B [25], the overall slope of $\ln[W(B)/W(0)]$ should be smaller than that of the theoretical curve which ignores activation (approximately, by a factor of 2, if we ignore the dependence of the activation rate on B).

A. The prefactor

The dependence of the potential $U(z)$ (38) on n gives rise to the density dependence of the tunneling rate $W(B)$ even for $B = 0$. We calculated the exponent and the prefactor in $W(0)$ by matching the WKB wave function under the barrier for $1/\gamma \ll z \ll L$ with the tail of the non-WKB intrawell solution (here, $L = \hbar^2 \gamma^2 / 2m|e\mathcal{E}_\perp|$ is the characteristic barrier width). In the spirit of the logarithmic perturbation theory (LPT) [26], the wave function of the ground state inside the well and not too far from it can be sought in the form

$$\psi_g(z) = \text{const} \times z \exp[-A(z)] \quad (40)$$

[we explicitly take into account that the function $\psi_g(z)$ has a zero in the ground state].

The function dA/dz satisfies a Riccati equation. It can be solved near the well ($z \ll L$) by considering the last two terms in the potential $U(z)$ (38) as a perturbation. For small z , the major correction comes from the term $\propto \mathcal{E}_\perp$. To the first order in \mathcal{E}_\perp ,

$$A(z) \approx \gamma z \left(1 - \frac{z}{4L}\right). \quad (41)$$

In obtaining this expression we took into account the correction to the ground state energy $\delta E_g = -3|e\mathcal{E}_\perp|/2\gamma$. This correction can be obtained from the condition that the linear in \mathcal{E}_\perp term in dA/dz remain finite for $z \rightarrow 0$.

The correction to A (41) is small for z small compared to the barrier width L . We note that the exponent $A(z)$ has an overall functional form which differs from that of the commonly used [2] variational wave function $\psi(z) \propto z \exp(-\tilde{\gamma}z)$, with $\tilde{\gamma}$ being the variational parameter.

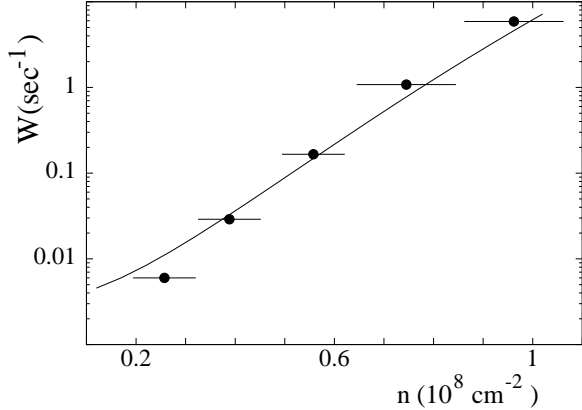


FIG. 9. The rate of electron tunneling from the helium surface $W(0)$ for $B = 0$ as a function of the electron density. The dots show the experimental data [5]. The pulling field \mathcal{E}_\perp was calculated from the geometry of the experimental cell, the applied voltage, and the density.

The expression for A (41) matches the small- z/L expansion of the action S of the WKB wave function under the barrier for $L \gg z \gg \gamma^{-1}$. This allowed us to find the prefactor in the WKB wave function and in the tunneling rate. The resulting tunneling rate is shown in Fig. 9. It fully agrees with the experiment (see also Ref. [20]).

VIII. CONCLUSIONS

It follows from the results of the present paper that interelectron momentum exchange in correlated 2D electron systems leads to an exponentially strong change of the rate of tunneling decay in a magnetic field parallel to the electron layer. The mechanism is dynamical by nature. It depends on the interrelation between the characteristic momentum exchange rate and the reciprocal duration of tunneling in imaginary time $1/\tau_f$.

For low temperatures, where escape occurs via tunneling from the ground state, the tunneling rate is affected primarily by high-frequency in-plane electron vibrations. In their turn, these vibrations are determined by short-range order in the 2DES. Their frequencies are of the order of the characteristic zone-boundary frequency of the Wigner crystal ω_p . If $\omega_p \gg 1/\tau_f$, the effect of the magnetic field on tunneling is nearly completely compensated in the case where the width of the tunneling barrier is small compared to the interelectron distance.

At higher temperatures, the magnetic field may in fact *enhance* rather than suppress the rate of tunneling decay. The overall escape rate as a function of B and T is expected to display a number of other unusual features. These include switching from activated escape to tunneling and vice versa, and switching between tunneling from the ground and excited states. These switchings have been analyzed for simple but realistic models of the tunneling barrier.

Our results on the field dependence of the tunneling rate and its evolution with temperature are in full qualitative and quantitative agreement with the existing experimental data on tunneling from a strongly correlated 2DES on helium [5], with no adjustable parameters.

The results also apply to 2DES in semiconductor heterostructures. For correlated systems in semiconductors, tunneling has been investigated mostly for the magnetic field \mathbf{B} perpendicular or nearly perpendicular to the electron layer, cf. [3]. The data on tunneling in a field parallel to the layer refer to high density 2DESs [27], where correlation effects are small.

The effect of a parallel magnetic field is most pronounced in systems with shallow and broad barriers $U(z)$. For example, in a GaAlAs structure with a square barrier of width $L = 0.1 \mu\text{m}$ and height $\gamma^2/2m = 0.02 \text{ eV}$, for the electron density $n = 1.5 \times 10^{10} \text{ cm}^{-2}$ and $B = 1.2 \text{ T}$ we have $\omega_p\tau_0 \approx 0.6$ and $\omega_c\tau_0 \approx 1$ ($\tau_0 = mL/\gamma$ is the tunneling duration for $n = B = 0$). The results of Sec. VI C for square barriers (with account taken of the correlation-hole correction) show that the interelectron momentum exchange should significantly modify the tunneling rate in this parameter range, provided the 2DES is correlated [29]. We therefore expect that tunneling experiments on low-density 2DESs in parallel fields will reveal electron correlations not imposed by the magnetic field, give insight into electron dynamics, and possibly even reveal a transition from an electron fluid to a pinned Wigner crystal with decreasing n .

We are grateful to B.I. Shklovskii for a helpful discussion. This research was supported in part by the NSF through Grant No. PHY-0071059.

-
- [1] E. Abrahams, S.V. Kravchenko, and M.P. Sarachik, cond-mat/0006055
 - [2] *Two-Dimensional Electron Systems on Helium and other Cryogenic Substrates*, ed. by E. Andrei (Kluwer, NY 1997).
 - [3] Presumably, correlations played a very substantial role in the giant increase of inter-layer tunneling observed recently in double layer heterostructures by I.B. Spielman *et al.*, Phys. Rev. Lett. **84**, 5808 (2000).
 - [4] *Perspectives in Quantum Hall Effects*, ed. by S. Das Sarma and A. Pinczuk (Wiley, NY 1997).
 - [5] L. Menna, S. Yücel, and E.Y. Andrei, Phys. Rev. Lett. **70**, 2154 (1993). E.Y. Andrei, in Ref. [2], p. 207.
 - [6] A strong effect on tunneling of the momentum transfer to defects was first discussed by B.I. Shklovskii, JETP Lett. **36**, 51 (1982); B.I. Shklovskii and A.L. Efros, Sov. Phys. JETP **57**, 470 (1983).
 - [7] J.S. Langer, Ann. Phys. (N.Y.) **41**, 108 (1967); S. Coleman, Phys. Rev. D **15**, 2929 (1977).

- [8] For a potential of a special form, the instanton technique was applied to tunneling of an electron coupled to harmonic oscillators in a magnetic field by P. Ao, Phys. Rev. Lett. **72**, 1898 (1994); Physica B **194-196**, 1233 (1994).
- [9] A.O. Caldeira and A.J. Leggett, Ann. Phys. (N.Y.) **149**, 374 (1983).
- [10] T. Barabash-Sharpee, M.I. Dykman, P.M. Platzman, Phys. Rev. Lett. **84**, 2227 (2000)
- [11] I. Affleck, Phys. Rev. Lett. **46**, 388 (1980)
- [12] A.I. Larkin and Yu.N. Ovchinnikov, Pis'ma Zh. Eksp. Teor. Fiz. **37**, 322 (1983) [JETP Lett. **37**, 382 (1983)]; J. Stat. Phys. **41**, 425 (1985).
- [13] C.C. Grimes and G. Adams, Phys. Rev. Lett. **42**, 795 (1979).
- [14] D.S. Fisher, B.I. Halperin, and P.M. Platzman, Phys. Rev. Lett. **42**, 798 (1979).
- [15] M.Ya. Azbel and P.M. Platzman, Phys. Rev. Lett. **65**, 1376 (1990).
- [16] R. P. Feynman and A. R. Hibbs, *Quantum Mechanics and Path Integrals* (McGraw-Hill, New York, 1965).
- [17] L.D. Landau and E.M. Lifshitz, *Quantum mechanics: non-relativistic theory* (Pergamon, NY 1977); M.V. Berry and K.E. Mount, Rep. Progr. Phys. **35**, 315 (1972).
- [18] U. Eckern and A. Schmid, in *Quantum Tunnelling in Condensed Matter*, eds. Yu. Kagan and A.J. Leggett (Elsevier, NY 1992), p. 145.
- [19] R. Landauer and Th. Martin, Rev. Mod. Phys. **66**, 217 (1994).
- [20] For $B = 0$, a good agreement between measured and numerically evaluated tunneling rates for electrons on helium was obtained by G.F. Saville, J.M. Goodkind, and P.M. Platzman, Phys. Rev. Lett. **70**, 1517 (1993).
- [21] M.J. Lea *et al.*, Phys. Rev. B **55**, 16280 (1997).
- [22] Y. Iye *et al.*, J. Low Temp. Phys. **38**, 293 (1980).
- [23] M.I. Dykman, J. Phys. C **15**, 7397 (1982).
- [24] S. Nagano *et al.*, Phys. Rev. B **19**, 2449 (1979).
- [25] The rate of activation escape may depend on the magnetic field, because the field “pushes” the ground state upward in energy, by $m\omega_c^2[\langle z^2 \rangle - \langle z \rangle^2]/2$, for a weak field (the averaging is performed for the ground state). Another factor is the change, by the magnetic field, of the wave functions with energies close to the barrier top. For $B = 0.4$ T the magnetic length $l = (\hbar c/eB)^{1/2}$ is ~ 0.6 of the distance from the helium surface to the barrier top position $(\Lambda/|e\mathcal{E}_\perp|)^{1/2}$. Both factors lead to the decrease of the activation energy of escape.
- [26] R.J. Price, Proc. Phys. Soc. London **67**, 383 (1954).
- [27] J.P. Eisenstein, T.J. Gramila, L.N. Pfeiffer, and K.W. West, Phys. Rev. B **44**, 6511 (1991); S.Q. Murphy, J.P. Eisenstein, L.N. Pfeiffer, and K.W. West, Phys. Rev. B **52**, 14825 (1995).
- [28] J. Smoliner *et al.*, Phys. Rev. Lett. **63**, 2116 (1989); G. Rainer *et al.*, Phys. Rev. B **51**, 17642 (1995).
- [29] M.I. Dykman, T. Sharpee, and P.M. Platzman, Phys. Rev. Lett. **86**, 2408 (2001).